Improved Thermal Stress Prediction in Quenched Cylindrical Bodies through a Dynamic Convection Coefficient Library

[1]P.L. Garrity, [1]K.L. Arthur and [2]D. Winkler
[1]*Naval Nuclear Laboratory, Knolls Atomic Power Lab, Advanced Structural Analysis Group, 2401 River Rd., Schenectady NY, 12309*
[2]*Dassault Systemes Simulia Corp., 1301 Atwood Ave., Suite 101W, Johnston RI, 02919*

Abstract: The transient temperature distribution of a quenched solid is driven by the convection coefficient at the wetted interface and the temperature difference between the component and quenching fluid. During finite element analysis, accurate applications of the convection coefficient is especially difficult due to the temporal evolution of the coefficient during the quenching process. For example, excursions through multiple regimes such as nucleate boiling followed by turbulent and/or laminar thermal boundary layers are common. During simulation efforts, a constant-valued coefficient is often used in lieu of the dynamic coefficient that accurately represents the convective boundary. Here we present the application of an automated convection library to a quenched cylindrical body. The library is an add-on package to Abaqus and runs within the standard Abaqus environment. The library contains numerous heat transfer correlations and transitions automatically between convection regimes as determined by dimensionless fluid numbers (Reynolds, Rayleigh, etc.). Moreover, temperature and pressure dependent properties are used and post processing visualization of all convection parameters are available in the Abaqus Visualization module. Our results are compared to a quenching analysis using a constant heat transfer coefficient. From the comparison, we show an improved prediction of lower residual stresses and a refined prediction of internal stress reversal.

Keywords: Quenching Heat Transfer, Thermal Stress, Residual Stress.

1. Introduction

Quenching is an essential step of heat treatment processes for steels and provides an avenue to control mechanical properties. In the quenching process, the steel is typically heated above the austenitizing temperature and subsequently cooled by immersion into a liquid bath or liquid spray. During the transient cool down, phase transformations occur resulting in a variety of microstructures, hardness and residual stress distributions, completely dependent on the temperature landscape within the material (Grossmann, 1964). Consequently, metallurgical property control is highly dependent on the heat flux and temperature distribution during this relatively short heat treatment step. Due to the large initial temperature difference between heated steel components and the quenchant, high heat fluxes ensue resulting in rapid cooling rates. Specifically, the temporal heat flux is determined by the time and spatially dependent heat transfer coefficient (HTC) at the wetted interface between the component and quenchant. This complex heat transfer problem has been investigated by other groups (Osman, 1990). With respect to simulations, convective boundary conditions for thermal analysis models are difficult to apply.

Depending on the component geometry, there may be localized areas of boiling while adjacent surfaces are below the fluid boiling point and are in the single phase natural convection regime. To address these challenges, many groups simply apply a conservative constant-value HTC (Wang, 1997 and Sen, 2000) due to the inability of finite element software to accommodate complex dynamic HTC's. Unfortunately, this practice results in inaccurate predictions of material phase transformations and residual stresses (Klinzing, 1992). Furthermore, conservative constant-valued HTC's usually predict excessive stress concentrations and probable cracking failure (Sen, 2000) due to thermal shock that persists throughout the cooling cycle. Here we present a novel methodology to apply HTC boundary conditions within Abaqus/Standard and a dynamic convection library extension.

Typically, the HTC is a function of fluid flow rate, fluid properties and dimensionless parameters such as Rayleigh (*Ra*), Reynolds (*Re*) and Prandtl (*Pr*) numbers. In addition, it is often dependent on surface properties such as geometry type, geometry orientation, roughness, and contamination. Many empirical formulas exist for dealing with different situations (Incropera, 1996). To complicate matters, due to the state dependencies, implementation of these formulas can make a solution highly nonlinear. In addition, automatically transitioning the HTC from one fluid regime to another (i.e., laminar to turbulent) can introduce significant HTC discontinuities which can make solution convergence very difficult.

This work utilizes a dynamic convection coefficient library packaged in an Abaqus/Standard extension. The extension affects behavior of all three process groups: solver, kernel, and GUI. It coexists with existing Abaqus/Standard functionality, while providing a relatively easy way for the user to prescribe convection coefficients at surfaces. Basically, the analyst's task of coding the complicated state-based HTC dependencies is eliminated. Convection correlation equations for various geometries reside within the library and are organized under catalog numbers.

For each thermal interaction that is activated by the user, HTC values are calculated at every surface flux point. Therefore, the HTC values may naturally evolve in space as well as time. For typical industrial applications there might be dozens of different surfaces in a finite element model that interface with a convective boundary. For transient solutions involving thousands of nodes on each surface, the proper HTC value could not possibly be prescribed without this type of automated approach. Incorporating a general purpose dynamic convection coefficient library becomes quite practical given the existence of a well-accepted collection of convection correlations.

A fluid property library is embedded in the extension to address dependencies on temperature and pressure for water, helium, and air for both SI and English units. Properties are calculated at each surface flux point and together with user prescribed fluid velocity, dimensionless fluid numbers are also calculated. All information is made available as user output.

Depending on the availability of known data, there may be several correlation equations that correspond to each catalog number in the convection coefficient library. This allows for dependencies on fluid number, evolving orientations (up-facing, down-facing), and activation/deactivation of local geometric dependencies (such as distance from leading edge of the flow). Additionally, the standard correlation equations for laminar and turbulent conditions may automatically transition to fluid conduction or nucleate boiling conditions. Equations may also be augmented with an equivalent conductance that is associated with a thin layer of material (such as insulation or coatings).

The convection library is maintained in a single text file that can be easily modified. Wherever possible, the logic that is associated with the applicability of each equation is also incorporated into the library. This includes things such as equation tolerances, valid fluid number ranges, and fluid number ranges of the known transition regions.

In the extension, the convection interactions architecture is similar to the Abaqus/Standard built-in film interactions, in the sense that they are all step-dependent and maintain a reference to an interaction property, i.e., film coefficient, which is not step dependent. As an enhancement over the built-in functionality of Abaqus/Standard, interactions may be activated and deactivated during any modeling step, and the properties of each thermal interaction can also be replaced during any step.

For the case where a correlation equation has not been established in the library, a thermal interaction property may be defined by a custom user equation. In addition, an interaction property can be created as a functional combination of existing interaction properties.

In summary, the convection library capability enables time and spatial dependency for a finite element thermal model resulting in accurate heat flux and temperature profiles relevant to quenching investigations. Accordingly, material phase transformation and residual stresses are better defined. The primary objective of this work is use Abaqus/Standard and the dynamic convection library to predict refined thermal stresses for a solid steel cylinder during a water quench. The temperature distribution is obtained first followed by mapping on to a structural model where the residual stress distribution is characterized. Both thermal and structural results are compared to published results of an identical steel cylinder analyzed with a constant-value HTC (Sen, 2000). Section 2 provides details of the thermal and structural analysis models and the comparative analysis focusing on variations and differences of all results are included in Section 3. The conclusion of this report is contained in Section 4.

2. Analysis Models

2.1 Finite Element Thermal Model

The objective of this section is to provide details of the Abaqus/Standard thermal model running the dynamic convection library extension. For comparative analysis purposes, this model contains identical 2D axisymmetric geometry, mesh density, element type (quadratic DCAX8), material and quenchant parameters as the published report (Sen, 2000). The cylindrical sample shown in Figure 1 is made of SAE 1020 steel and measures 0.030 m long with a diameter of 0.010 m. Due to symmetry, the one-quarter axisymmetric model contains 121 quadratic elements and 408 nodes. The mesh size is biased identically to the comparative model (Sen, 2000). The model dimensions are l = 0.015 m long and r_O = 0.005 m. Point O shown in Figure 1 is the center of the solid cylinder while points K, L and M are located on the cylinder outer surface.

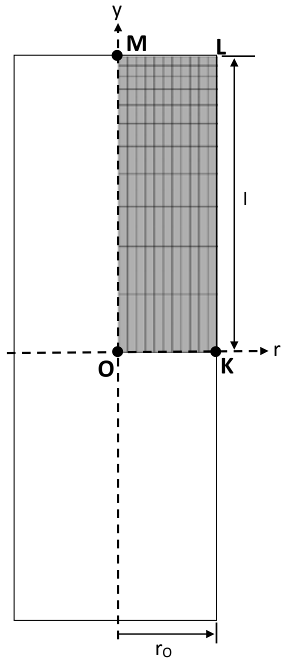

Figure 1. Geometry and axisymmetric finite element model of the SAE 1020 steel cylinder.

The mechanical and thermal properties identical to the comparative model are shown in Table 1. It is evident that temperature dependent properties were not used for all modeling inputs. The Abaqus/Standard analysis duplicated all properties shown in Table 1 in order to accomplish the comparative analysis.

Table 1. Mechanical properties of SAE 1020.

Temp (˚C)	Thermal Conductivity (W/m-K)	Specific Heat (J/kg-K)	Density (kg/m^3)	Thermal Expansion Coefficient ($˚C^{-1}$)	Poisson's Ratio	Yield Strength (MPa)	Modulus of Elasticity (MPa)	Modulus of Plasticity (MPa)
20	43.124	579.7	7800	1.41×10^{-4}	0.30	256	210×10^3	3.63×10^3
100	43.124	579.7	7800	1.41×10^{-4}	0.30	221	206×10^3	3.4×10^3
200	43.124	579.7	7800	1.41×10^{-4}	0.30	216	200×10^3	3.32×10^3
400	43.124	579.7	7800	1.41×10^{-4}	0.30	157	181.5×10^3	3.0×10^3
600	43.124	579.7	7800	1.41×10^{-4}	0.30	73	165×10^3	0.8×10^3

The following assumptions have been made for the thermal model:

- The quenching process occurs at atmospheric pressure.
- The steel cylinder initial temperature is 600 ˚C.
- The water bath quenchant is large enough to act as a sink and remains at 20 ˚C throughout the cooling cycle.
- Latent heat released during steel phase transformations is negligible and ignored.
- The steel surface is smooth and does not enhance boiling heat transfer.
- The steel surface condition is assumed oxidized upon immersion into the quenchant resulting in an emissivity of 0.7 (Incropera, 1996).

During the quenching process, the relationship between the component surface heat flux and temperature undergoes extreme changes. As shown in the water boiling curve of Figure 2, changes are driven primarily by evolution of the mechanism of liquid water and water vapor contact with the component surface. The important parameters in the boiling curve are the component wall temperature T_W, water saturation temperature T_{sat} (100 ˚C for this analysis) and the associated heat flux q'' corresponding to the excess wall temperature $\Delta T_E = (T_W - T_{sat})$. Various interfacial regimes are transited during cooling in a stagnant water bath. During the initial moments of the quench, the hot surface induces film boiling (Figure 2, point E) where a vapor blanket separates the water from the surface. Heat transfer occurs by conduction and radiation through the vapor blanket from the surface to the liquid water. The minimum heat flux occurs at point D due to reduced radiation. Collapse of the vapor layer begins thus promoting liquid water wetting of the surface and the transition boiling regime. The transition boiling region between points D and C is characterized by a substantial increase in the heat flux. The critical or maximum heat flux occurs at point C where the entire component surface becomes available for nucleate boiling. Nucleate boiling diminishes between points B and A transitioning to single phase natural convection (NC) below point A. It is important to point out that the NC regime may begin with a turbulent thermal boundary layer at point A and transition to a laminar boundary layer as ΔT_E reduces. In order to simulate the various convection regimes shown in Figure 2, three analysis Steps were created in Abaqus/Standard. The HTC was obtained at discrete points between E and

D and again between D and C by calculating the HTC h_B from the governing heat flux equation for boiling $q" = h_B(T_W - T_{sat})$ (Incropera, 1996). From this data, a tabular amplitude table of HTC's as a function of T_W was created within Abaqus/Standard. Table 2 below gives the calculation results. Step 1 of the Abaqus/Standard model included the tabular HTC's from the boiling curve in addition to radiation from the steel cylinder surface to a 20 ˚C (water) sink. Step 2 incorporates the tabular HTC's from the boiling curve with no radiation due to the water vapor blanket collapse. Step 3 utilizes the dynamic convection library extension.

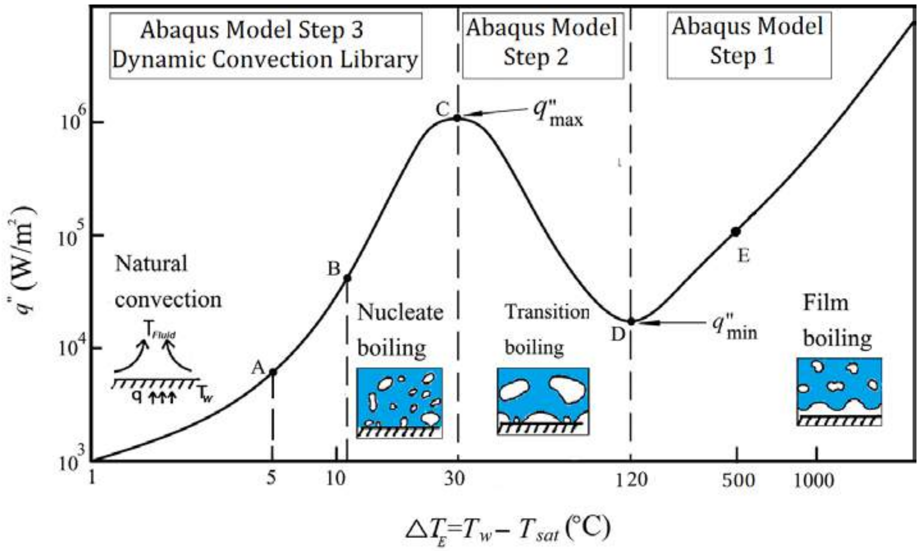

Figure 2. Water boiling curve at atmospheric pressure. The Abaqus/Standard model was run in 3 Steps in order to simulate radiation, two-phase convection and single-phase convection.

Table 2. Steel cylinder film and transition boiling HTC's as a function of cylinder wall temperature T_W. The temperature dependent HTC's were applied to the Abaqus/Standard model in Steps 1 and 2 only. For T_W < 130 ˚C, HTC's were applied by the dynamic convection library.

T_W (˚C)	130	150	200	250	300	320	400	500	600
Heat Transfer Coefficient (W/m² ˚C)	33852.4	9290.3	287.2	210.8	141.2	86.5	489.6	567.1	632.5

The HTC for vertical cylinders was selected from the convection library. The convection library calculates turbulent and laminar HTC's from the following correlations (Incropera, 1996):

$$Nu = \frac{hL}{k} = \left\{ 0.825 + \frac{0.387 Ra^{1/6}}{\left[1 + \left(0.492/\Pr\right)^{9/16}\right]^{8/27}} \right\}^2 \qquad 10^9 \le Ra \le 10^{12} \quad \text{(Turbulent)},$$

(1)

$$Nu = \frac{hL}{k} = 0.680 + \frac{0.670 Ra^{1/4}}{\left[1 + \left(0.492/\Pr\right)^{9/16}\right]^{4/9}} \qquad 0 \le Ra \le 10^9 \quad \text{(Laminar)},$$

(2)

where L is the characteristic material length and k is the fluid thermal conductivity. During runtime, the convection library calculates Ra, Pr and h at each increment from user inputs of L, water temperature and water pressure. Transition between turbulent and laminar regimes is executed automatically on a nodal basis during runtime. Under the conditions where $T_W > T_{Fluid}$ and $T_W > T_{sat}$, the convection library automatically transitions to the nucleate boiling correlation (Rohsenow, 1998):

$$\Delta T_E = 25 q^{"0.25} \exp(-P/62),$$

(3)

where the nucleate boiling heat flux $q" = h_{NB}(T_W - T_{sat})$ is in MW/m^2 and the pressure P is in bars. The convection library calculates h_{NB} from known values of the other variables during runtime.

A summary of all boundary conditions applied to the steel cylinder and transient run times are shown in Table 3. A separate validation model was used to confirm the Abaqus/Standard results with the constant-value HTC (Sen, 2000). Details of the separate model is given in Section 3.1.

Table 3. Abaqus/Standard thermal model boundary conditions summary. The transient time period for each step is shown in parentheses.

Boundary Condition	Step 1 (0 – 36 sec)	Step 2 (36-42 sec)	Step 3 (42-120 sec)
Radiation	Yes	No	No
Temperature Dependent HTC (Abaqus/Standard)	Yes	Yes	No
Dynamic Convection Library HTC for Vertical Cylinder Geometry	No	No	Yes

2.2 Finite Element Structural Model

The structural model uses Abaqus/Standard to calculate the residual stresses based on the temperature distribution from the thermal model. The structural model uses the same geometry, mesh density, and material as the thermal model as shown in Figure 1. The structural model consisted of 121 quadratic, eight node structural axisymmetric elements of Abaqus type CAX8.

Owing to the symmetry of the quarter model, the OK edge was restricted from displacing vertically and the displacement along the OM edge was restricted in the radial direction. The material is assumed to possess elastic-plastic behavior using the isotropic hardening model (Abaqus, 2016) with the inputs from Table 1

3. Results and Discussion

3.1 Thermal Analysis Results

In order to complete a comparative analysis between the quenched cylinder using a constant-valued HTC (Sen, 2000) and the convection library described herein, a separate validation model was assembled in Abaqus/Standard. This model duplicated all mechanical properties (see Table 1) and had length $l = 0.075$ m and $r_o = 0.050$ m. A constant HTC of 16742.2 W/m^2 ˚C was used identical to the comparison model solved in ANSYS (Sen, 2000). Figure 3 shows the temperature comparison at identical locations (see Figure 1) between Abaqus/Standard and ANSYS (Sen, 2000). Good agreement is found between the two models with deviations attributed to the age difference between the two solvers. The thermal response agreement lends credibility to the comparative analysis and establishes a finite element modeling baseline to assess changes in thermal stresses.

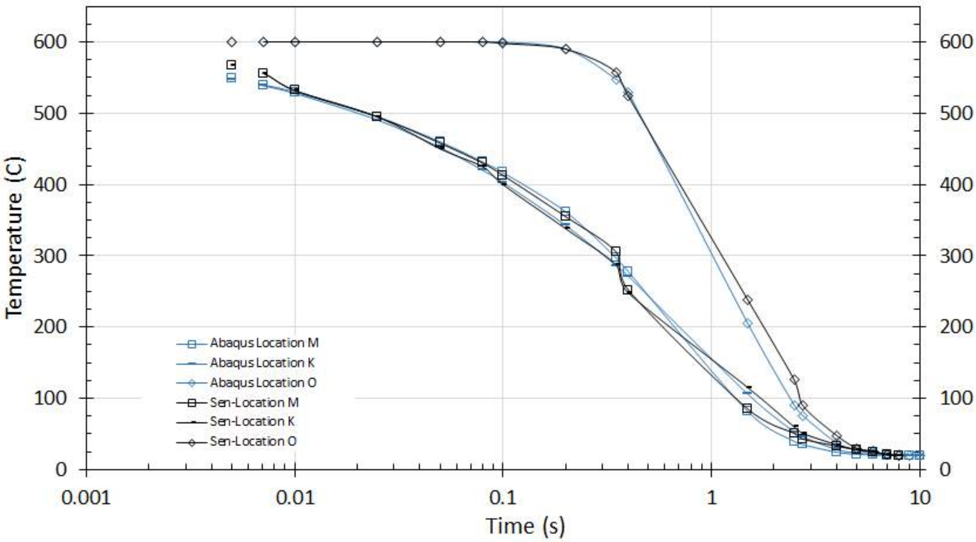

Figure 3. Validation results for the comparative temperature response between Abaqus and the baseline model solved in ANSYS (Sen, 2000).

Figure 4 below shows the comparative temperature decay between the constant-valued baseline HTC (Sen, 2000) and the convection library model defined in Figure 1 and Table 1 of this report. The baseline model used a constant HTC of 16742.2 W/m^2 ˚C throughout the quench cycle while the convection library model used the boundary conditions described in Section 2.1. The comparative temperature locations are shown in Figure 1 and substantial differences are found between the two models. At 1 second, the baseline model predicts a cylinder top surface temperature (point M) of approximately 90 ˚C while the convection library model predicts approximately 585 ˚C at the same location. A temperature difference between the cylinder surface and core of approximately 260 ˚C is predicted for the baseline model at 1 second while the convection library model predicts 10 ˚C. The large thermal gradient between the cylinder surface and core is due entirely to excessive thermal shock which is unrealistic due to the vapor blanket known to form between the surface and fluid at this stage of water quenching (Klinzing, 1992). It is interesting to note the convection library model predicts nucleate boiling for 3 seconds (42 – 45 seconds) followed by turbulent NC for 42 seconds (45 – 87 seconds) followed by laminar NC for the remaining 33 seconds. Furthermore, nucleate boiling is found to cease at the cylinder upper right corner first followed by diminished boiling at Point M and K a short time later. This behavior is expected due to cylinder edge effects inducing faster cooling than cylinder side/top walls. The baseline model also predicts complete cool down in less than 6 seconds while the convection library model predicts approximately 105 seconds to approach the quenchant temperature.

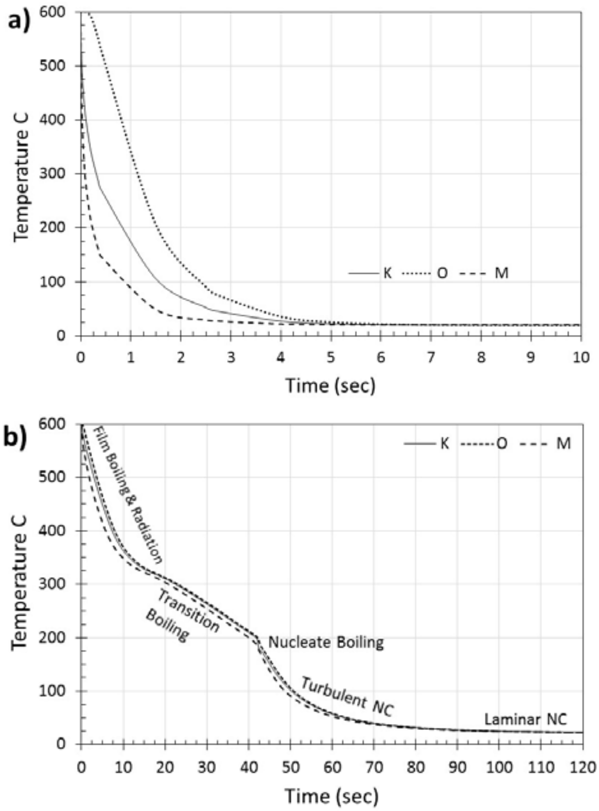

Figure 4. Temperature response for the baseline ANSYS model (Sen, 2000) and the Abaqus/Standard model incorporating the convection library. a) A constant HTC of 16742.2 W/m^2 ˚C was used in this model throughout the quench cycle. b) HTC's corresponding to each boiling regime followed by turbulent and laminar NC were applied during the quench cycle.

Figure 5 compares the constant-value HTC (Sen, 2000) compared to the convection library HTC at point K. Boiling and NC regimes elucidate the peaks and valleys of the quenching process. The relatively low HTC during film boiling is only 3.6% of the constant-value HTC and the minimum value at approximately 18 seconds corresponds to the minimum heat flux (see Figure 2). The short time spent in nucleate boiling is notable and is due to the large HTC inducing significant heat removal driving ΔT_E below 5 ˚C. Turbulent and laminar NC HTC's steadily decline as expected due to the reducing *Ra* number.

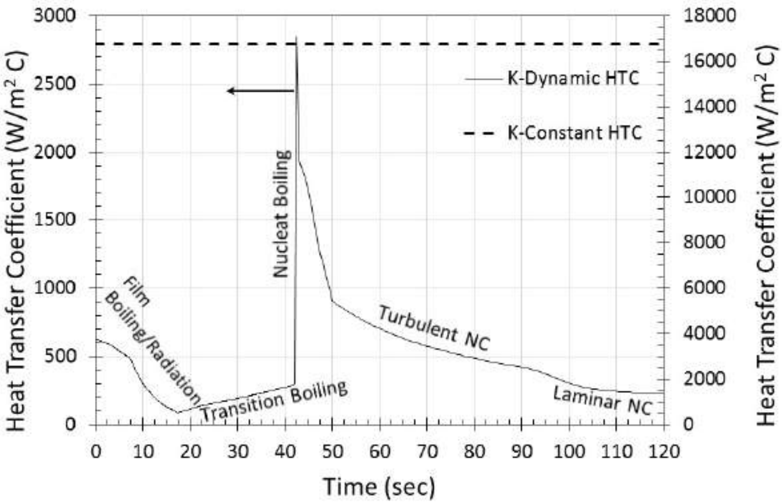

Figure 5. Comparison of the constant-value HTC (16,742.2 W/m^2 ˚C) to the dynamic HTC applied by Abaqus/Standard and the convection library.

Figure 6 shows the spatial distribution of the convection library HTC at 44.5 seconds. During this time point, nucleate boiling was present on the side and top-center cylinder walls however the upper corner temperature at point L cooled to the point of transition into turbulent NC ($T_W < T_{sat}$). Consequently, the presence of mixed convection evolving spatially is captured resulting in remarkable HTC granularity.

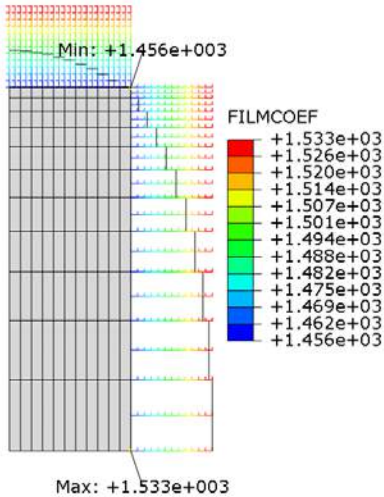

Figure 6. Spatial distribution of the convection library HTC at 44.5 seconds. The HTC's applied by the convection library include nucleate boiling at the cylinder side and top/center walls while turbulent NC is applied at the cooler upper tight corner point L due to $T_W < T_{sat}$.

Figure 7 provides comparative details of the steel cylinder heat flux. The plot includes the initial heat flux at the beginning of the quench for the constant-value HTC (9.01 x 10^6 W/m^2) and the peak heat flux for the convection library HTC (1.85 x 10^6 W/m^2). According to the water boiling curve shown in Figure 2, a heat flux of 9.01 x 10^6 W/m^2 would require a ΔT_E much greater than 1,000 ˚C which is unrealistic given the initial cylinder temperature of 600 ˚C. Accordingly, the heat flux decays to near zero in approximately 5 seconds due to the excessive thermal shock. The heat flux for the Abaqus/Standard model evolves similarly to the HTC (Figure 5) which is considered reasonable due to the functional dependence of the heat flux to ΔT_E for water at atmospheric pressure.

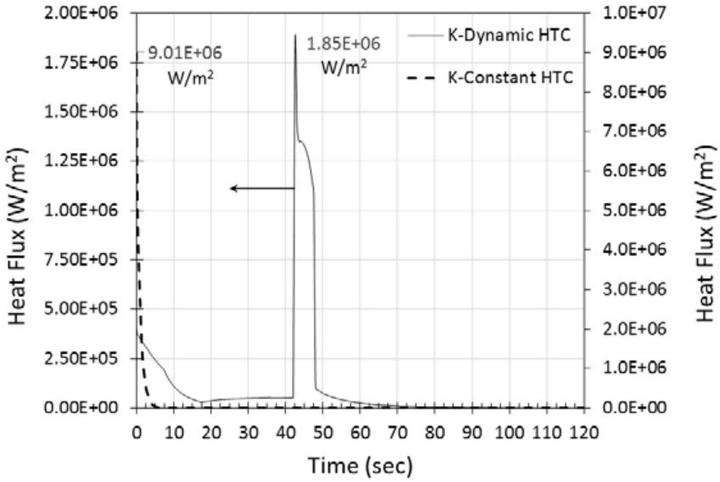

Figure 7. Comparison of the baseline model (Sen, 2000) and Abaqus/Standard model heat flux.

3.2 Structural Analysis Results

The residual stresses resulting from a constant-valued HTC using Abaqus/Standard were compared with the stresses from a constant-valued HTC (Sen, 2000). The distribution of residual stress with time during water quenching through the points M, K and O is shown in Figure 8a. The radial and axial stresses, σ_r and σ_y, at the points M, K and O show similar trends and increase with the increasing time and are tensile at early stages of cooling and then become compressive after 0.3 s which is the same as constant-valued HTC model (Sen, 2000). The difference in residual stress at several times throughout quenching between the constant-valued HTC model (Sen, 2000) and the Abaqus/Standard constant-valued HTC model is attributed to the difference in plasticity models. Figure 8b shows the radial, axial and tangential stress variations with the inner-radial surface along the OK line at the end of quenching from the constant-value HTC model (Sen, 2000) and the Abaqus/Standard constant-valued HTC model. Both models show that the radial stress, σ_r, is tensile at the center axis and then shifts to a zero stress state at the surface of the cylinder. The stress components σ_y and σ_θ are compressive close to the surface but change to tensile at the center of the cylinder.

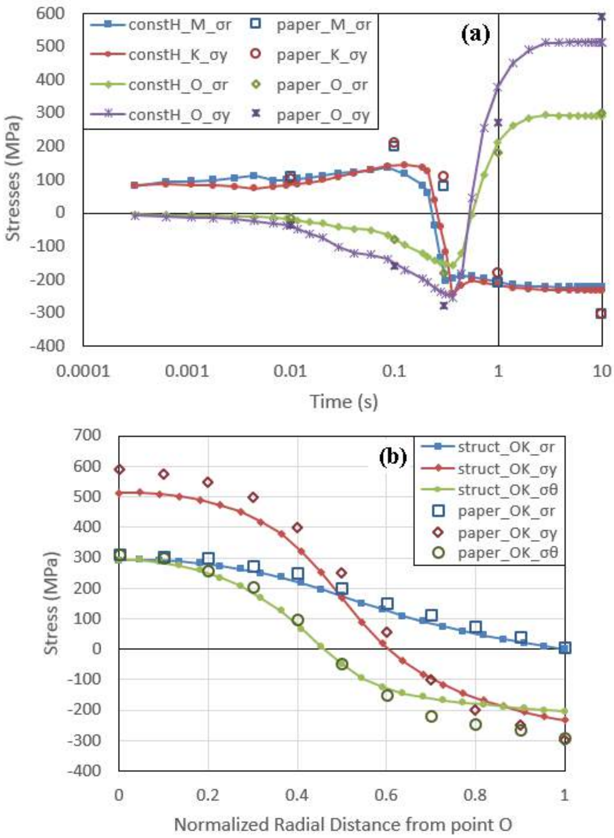

Figure 8. Comparison of constant-valued HTC from literature (Sen, 2000) and Abaqus/Standard for (a) the relationship between residual stress and quenching time and (b) the variation of residual stress along the OK line at end of quenching.

The previous comparisons qualify the Abaqus/Standard structural model for a constant-valued HTC so it can now be used to produce the residual stresses due to the temperature distribution from the convective library model. Similar comparisons at the same locations are described and demonstrate the residual stress difference due to a constant-valued HTC versus using the convective library model. The distribution of residual stress with time during water quenching through the points M, K and O is shown in Figure 9. The radial and axial stresses, σ_r and σ_y, at the points M and K show similar trends and are tensile at early stages of cooling and transition to compressive stresses. The convective library model's stresses become compressive at a slower rate than the constant-valued HTC model. Both models at points M and K reach a similar compressive final stress. The radial and axial stresses, σ_r and σ_y, at point O show greater differences between the two models. Both models start off compressive and then transition to tensile at similar times throughout the quenching process. The transition from compressive to tensile stress occurs more gradually in the convective library model compared to the constant-valued HTC model. The convective library model tensile stresses at point O are significantly lower than the constant-value HTC at the end of quenching. This results in a lower overall residual stress state at point O.

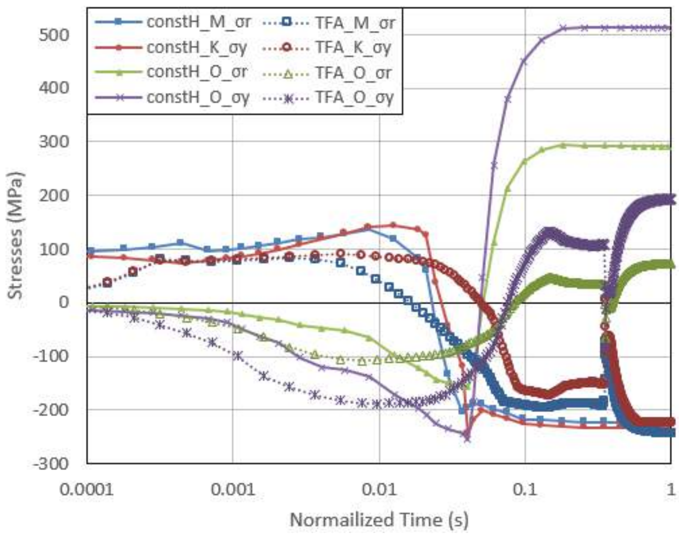

Figure 9. Comparison of relationship between residual stress and quenching time for constant-valued HTC and convective library model.

The stress variation along frontal surface line KL at the end of quenching remains mostly compressive as shown in Figure 10a for axial σ_y and tangential stress σ_θ. As can be seen from Figure 10a, the axial residual stress values stay fairly constant throughout the wall thickness. This trend continues across the majority of the path's thickness. At roughly 4/5 of the path's thickness, the axial stress σ_y approaches zero sharply and reaches a zero stress state at the frontal surface. The tangential stress σ_θ shows very little stress difference throughout the length of the frontal surface. Figure 10b shows the radial, axial, and tangential stress variations with the inner-radial surface along the OK line at the end of quenching comparing residual stresses from a constant-valued HTC and convective library model. The axial σ_y and tangential stress σ_θ are tensile at the center of the cylinder at point O and shifts to compressive at the surface at point K. The convective library model axial and tangential stresses start at a lower tensile stress at point O and transition to compressive at a slower rate but end of at the same compressive stress magnitude at point K. The radial stress σ_r remains tensile along the inner-radial surface (OK edge). The convective library model radial stress starts at a lower tensile stress at point O but decreases to a zero stress state at point K like the constant-valued HTC. Figure 10b shows the large residual stress difference at the center of the cylinder between the constant-valued HTC model and convective library model.

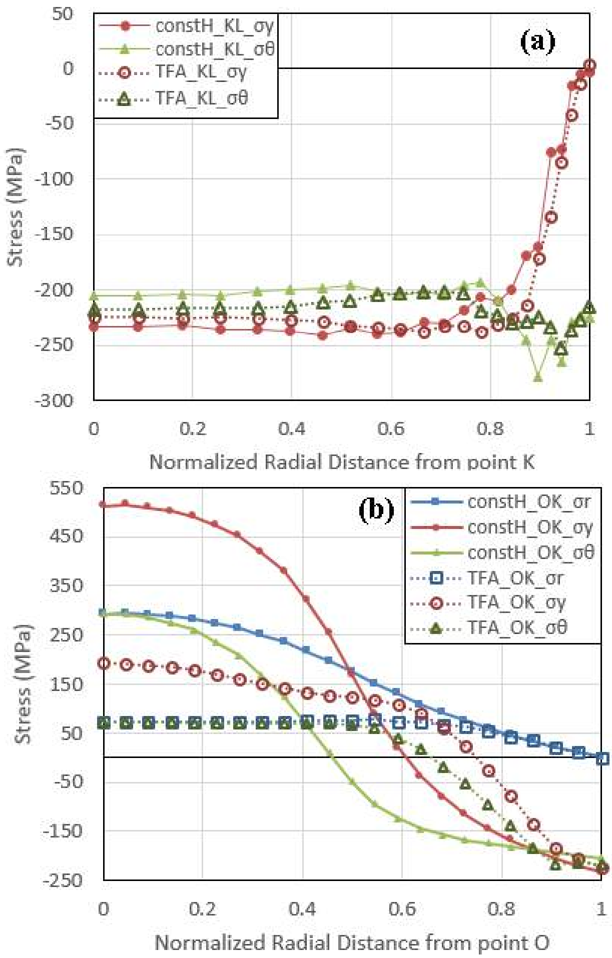

Figure 10. Variation of Residual Stress due to a constant-valued HTC and convective library model at End of Quenching along the (a) KL line and (b) OK line.

Figure 11 shows the maps of (a) residual Von Mises stress at the beginning of cooling and (b) axial residual stress at the end of cooling for a constant-valued HTC and convective library model. From the maps it can be seen that the effective stress remains highest near the cooling surfaces and is lower in the center of the cylinder for both the constant-valued HTC and the convective library model. Figure 11a shows that although they have similar stress distributions, the convective library model has half the stresses of the constant-valued HTC. The convective library model also shows significantly lower tensile axial stresses compared to the constant-valued HTC model as shown in Figure 11b. The constant-valued HTC model also shows that the compressive stresses along the cooling surfaces permeate the interior of the cylinder further than the convective library model. The convective library model shows a more even distribution from compressive stress to tensile stresses at the center of the cylinder compared to the constant-valued HTC model which has very high tensile stresses a small distance below the upper radial surface.

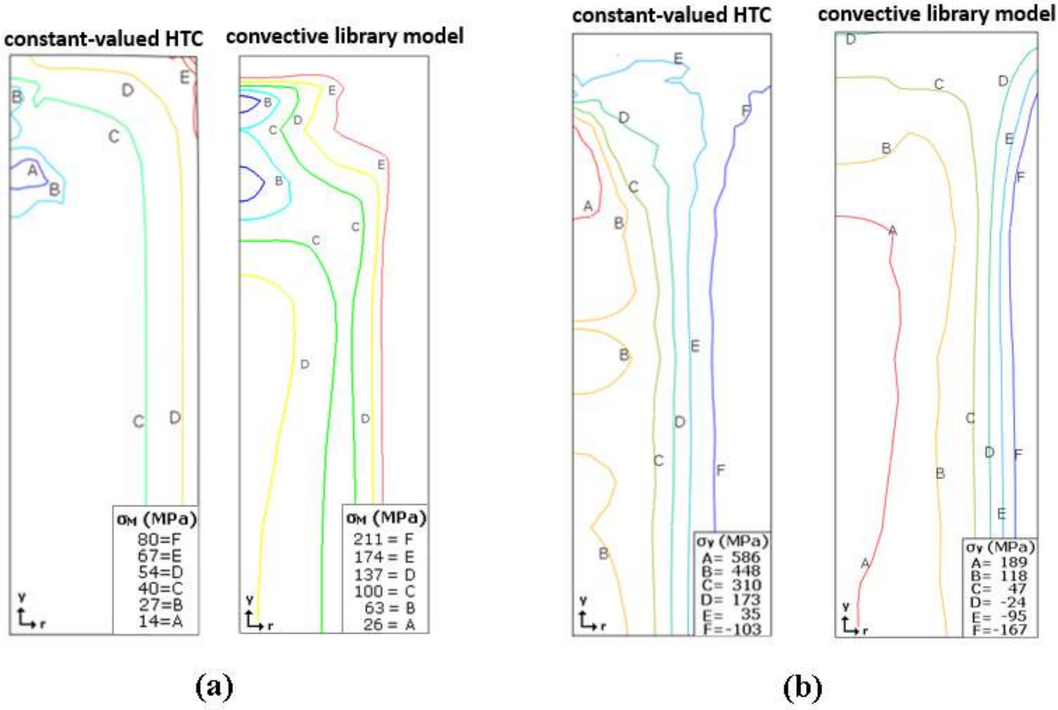

Figure 11. Residual stress distribution maps for steel solid cylinder at (a) beginning and (b) end of water quenching for a constant-valued HTC and convective library model.

4. Conclusion

Finite element analysis of residual thermal stresses of a steel cylinder undergoing water quenching has been performed with a specific analysis focus on the HTC. A constant-value HTC of 16742.2 W/m^2 °C based on prior results (Sen, 2000) was compared to a convection library that applied HTC's on a nodal basis in a spatial and transient manner. The multi-Step model utilized temperature dependent HTC's obtained from the standard water boiling curve for Steps 1 and 2. The convection library was initiated in Step 3 and was found to correctly apply nucleate boiling HTC's followed by automatic transition to turbulent NC and finally, laminar NC. The comparative analysis elucidated important differences in the thermal profile of the cylinder that directly influence downstream structural investigations. For example, temperature differences between the cylinder surface and inner core are predicted to be far less than conservative constant-value HTC's. Additionally, geometrical features often show different transient temperature profiles when compared to adjacent surfaces. In this work, the cylinder corners are predicted to cool below the water boiling point before the cylinder side and top walls. The convection library appropriately applied the HTC for single phase turbulent NC to this area while simultaneously applying the HTC for nucleate boiling to nodes above T_{sat}. The structural results show that the convection library produce lower effective stresses than the constant-valued HTC model. Both models show the same trend of residual stresses acting as compressive along the cooling surfaces and by moving away from the outer surface towards the center of the cylinder, the stresses decrease and reverse their sign to become tensile. The convection library reduces the distance into the thickness as to when the sign of the stress reverses as the effective stress goes to a minimum at a closer distance to the cooling surface compared to the constant-valued HTC model.

5. References

Abaqus Theory Guide, Version 2016, Dassault Systemes Simulia Corp., Providence, RI.

Grossman, M.A. and Bain, E.C., 1964, "*Principles of Heat Treatment*," American Society for Metals, Metals Park, OH.

Incropera, F.P. and DeWitt, D.P., 1996, 3rd ed., "*Introduction to Heat Transfer*," John Wiley & Sons, NY.

Klinzing, W.P., Rozzi, J.C. and Mudawar, I., "Film and Transition Boiling Correlations for Quenching of Hot Surfaces with Water Sprays," J. Heat Treating, **9** 91-103 (1992).

Osman, A.M. and Beck, J.V., "Investigation of Transient Heat Transfer Coefficients in Quenching Experiments," J. Heat Transfer, **112** 843-848 (1990).

Rohsenow, W.M., Hartnett, J.P. and Cho, Y.I., 1998, 3rd ed., "*Handbook of Heat Transfer*," McGraw Hill, NY.

Sen, S., Aksakal, B. and Ozel, A., "Transient and Residual Thermal Stresses in Quenched Cylindrical Bodies," Int. J. Mech. Sciences, **42** 2013-2029 (2000).

Wang, K.F., Chandrasekar, S. and Yang, H.T.Y., "Experimental and Computational Study of the Quenching of Carbon Steel," J. Manuf. Sci. Eng., **119** 257-265 (1997).

6. Acknowledgements

The authors wish to thank Mark Lansberry with Naval Reactors and Andrew Smith with BMPC Information Security for their valuable assistance with this project. The support of Ted Schurman managing the Advanced Structural Analysis Group and Senior Manager Paul Smith with Structural Technology is gratefully acknowledged.